crystals

MDPI

Article

Advanced Copper Oxide Chemical and Green Synthesis: Characterization and Antibacterial Evaluation

Ecaterina Magdalena Modan [1], Adriana-Gabriela Schiopu [2,*], Sorin Georgian Moga [1], Denis Aurelian Negrea [1], Daniela Istrate [3], Ion Ciuca [3] and Mihai Oproescu [4]

[1] Regional Center of Research & Development for Materials, Processes and Innovative Products Dedicated to the Automotive Industry (CRCD-AUTO), Pitesti University Centre, National University of Science and Technology Politehnica Bucharest, 060042 Bucharest, Romania; ecaterina.modan@upb.ro (E.M.M.); sorin_georgian.moga@upb.ro (S.G.M.); aurelian.negrea@upb.ro (D.A.N.)
[2] Faculty of Mechanics and Technology, Pitesti University Centre, National University of Science and Technology Politehnica Bucharest, 110040 Pitesti, Romania
[3] Doctoral School Materials Science and Engineering, National University of Science and Technology Politehnica, Splaiul Independentei No. 313, Sector 6, 060042 Bucharest, Romania; calin_istrate_daniela@yahoo.com (D.I.); ion.ciuca@upb.ro (I.C.)
[4] Faculty of Electronics, Communication and Computers, Pitesti University Centre, National University of Science and Technology Politehnica Bucharest, 110040 Pitesti, Romania; mihai.oproescu@upb.ro
* Correspondence: gabriela.schiopu@upb.ro

Abstract: Recent advancements in nanotechnology have improved the application of copper oxide (CuO) nanostructures, known for their diverse antibacterial, electrical, catalytic, optical, and pharmacological properties, which depend on nanoparticle morphology. This study investigated two synthesis methods for structured CuO: microwave-assisted hydrolysis and ultrasound using copper acetate and KOH, and an eco-friendly method involving cholesterol-free egg white albumin and *Solanum lycopersicum* extract. Characterization techniques, including XRD, FTIR, and SEM-EDS, were utilized to analyze the produced CuO. XRD confirmed high-purity monoclinic CuO structures in the sample obtained via the chemical method, while characteristic peaks of tenorite and dolerophanite were observed in the albumin-synthesized sample. ATR-FTIR analysis revealed O-H stretching bands around 3400 cm^{-1}, indicating adsorbed H-OH or -OH and strong Cu-O bond peaks at 434 cm^{-1}. The CuO synthesized via microwave and ultrasound methods displayed superior crystallinity compared to commercial CuO. SEM illustrated various morphologies, such as flakes, microspheres, and irregular polyhedra, influenced by the presence of proteins and organic acids. Antibacterial tests demonstrated the effective inhibition of *Escherichia coli* and *Enterococcus faecalis*, confirming the potential of CuO as a promising antibacterial agent. Overall, the findings highlight the effectiveness of green chemistry in developing crystalline CuO for various applications.

Keywords: nanostructured copper oxide; chemical synthesis; green synthesis; characterization; antibacterial tests

check for updates

Academic Editor: Qian Lei

Received: 10 December 2024
Revised: 21 December 2024
Accepted: 23 December 2024
Published: 25 December 2024

Citation: Modan, E.M.; Schiopu, A.-G.; Moga, S.G.; Negrea, D.A.; Istrate, D.; Ciuca, I.; Oproescu, M. Advanced Copper Oxide Chemical and Green Synthesis: Characterization and Antibacterial Evaluation. *Crystals* **2025**, *15*, 7. https://doi.org/10.3390/cryst15010007

Copyright: © 2024 by the authors. Licensee MDPI, Basel, Switzerland. This article is an open access article distributed under the terms and conditions of the Creative Commons Attribution (CC BY) license (https://creativecommons.org/licenses/by/4.0/).

1. Introduction

Nanotechnology has unlocked significant avenues in materials science, particularly in the development of metal oxide nanoparticles with unique physicochemical properties [1]. Nanostructured copper oxide (CuO) has garnered considerable interest in nanotechnology due to its multifunctional properties, spanning a wide range of applications from antimicrobial coatings and drug delivery systems to environmental technologies and catalysis [2–4]. In recent years, nanostructured CuO has exhibited remarkable antibacterial,

catalytic, electrical, and optical properties, stemming from its unique electronic structure and chemical reactivity [5]. This renders it a promising material for applications demanding high efficiency and versatility. These properties are significantly influenced by particle size, surface area, and nanostructure morphology, which can be finely tuned through the synthesis method [6]. The demand for CuO nanoparticles with tailored properties has spurred a broad range of synthetic approaches, including chemical, physical, and green methods [7]. Conventional synthesis methods such as sol–gel, precipitation, and hydrothermal processes can produce CuO with high purity and a controlled particle morphology [8–10]. However, they often involve high temperatures, pressures, and harsh chemicals, limiting their scalability and environmental sustainability [11].

Chemical synthesis methods employ a "bottom–up" strategy, which involves assembling simple units into more complex structures, ultimately resulting in the formation of nanoparticles (NPs) [12]. These approaches are cost-effective and facilitate the production of uniformly sized and shaped products on a large scale, without the need for high-capacity equipment. The sol–gel method is particularly suitable for synthesizing CuO nanoparticles due to its simplicity, scalability, and cost-effectiveness [13]. Recently, crystalline CuO nanoparticles with sizes ranging from 100 to 140 nm and an adjustable surface area have been produced using copper carbonate precursors at a pH of 5.8 and calcination temperatures exceeding 250 °C [14]. Additionally, Shanan et al. reported the synthesis of CuO nanoparticles measuring 77 nm by calcining a copper nitrate precursor at 200 °C for 2 h [15]. Phiwdang et al. developed a precipitation technique to produce CuO nanoparticles with various sizes and morphologies, starting from two distinct precursors: copper nitrate and copper chloride [16]. In other studies, CuO nanoparticles were synthesized using several precursors, including copper(II) sulfate, chloride, and acetate, generating particles of various shapes and sizes [16]. Furthermore, Pookmanee et al. developed nanostructured copper oxide using a microwave method, applying an irradiation power of 600–800 W for 6 min; the resulting particles exhibited an irregular and agglomerated shape, with average sizes ranging from 350 to 670 nm [17].

The increasing demand for environmentally friendly materials and sustainable synthesis processes has stimulated research into alternative, energy-efficient techniques that minimize environmental impact without compromising quality or functional properties [18]. Recent advances in microwave- and ultrasound-assisted synthesis have emerged as efficient alternatives due to their energy efficiency, rapid reaction times, and ability to control nanoparticle morphology [19,20]. For example, microwave synthesis uses electromagnetic radiation to uniformly heat the reaction medium, resulting in faster rates of nucleation and particle growth [21]. This technique is particularly advantageous in the synthesis of metal oxide nanoparticles, as it provides fine control over particle size, crystallinity, and phase purity [22]. Ultrasound-assisted synthesis employs ultrasonic waves to generate high-energy cavitation, which significantly accelerates chemical reactions and facilitates uniform particle dispersion [23]. This method is instrumental in the production of nanoparticles, resulting in smaller and more consistent particle sizes. The enhanced kinetic environment provided by ultrasonic waves not only improves reaction efficiency but also ensures the homogeneity of the resultant nanomaterials [24]. These synthesis methods not only offer greater energy efficiency but also provide better control over particle morphology, making them suitable for applications where specific particle characteristics are required [25]. In addition to physical and chemical methods, green synthesis approaches have gained attention due to their sustainability and potential for biocompatibility [26].

Green synthesis often involves natural plant extracts, proteins, or biological agents as stabilizing and reducing agents, thereby reducing or even eliminating the need for toxic chemicals [27]. Such methods align well with the principles of green chemistry, which

emphasize the use of non-toxic materials, waste reduction, and the minimization of energy consumption [28]. Plant extracts, for example, provide a rich source of antioxidants, organic acids, and proteins that can act as effective reducing agents to promote the formation of nanoparticles [29].

The green synthesis of nanostructured oxides has attracted significant interest due to their environmentally friendly and cost-effective nature. This approach utilizes natural non-toxic materials, such as plant extracts and microorganisms, as reducing agents, thus minimizing the environmental impact compared to traditional methods which often rely on hazardous chemicals. Green synthesis is considered a sustainable, biocompatible, and eco-friendly alternative for the large-scale production of nanoparticles, addressing concerns related to toxicity and pollution associated with conventional synthesis techniques. However, like any scientific approach, it presents both advantages and challenges.

Tables 1 and 2 present a summary of the main advantages and disadvantages of green synthesis methods for producing nanoparticles. These methods are evaluated based on their environmental impact, cost-effectiveness, simplicity, scalability, and ability to control nanoparticle properties, as well as the challenges related to uniformity, reaction rates, and the extraction of natural reducing agents.

Table 1. Advantages of green synthesis.

Advantages of Green Synthesis	Description	References
Environmentally Friendly	Green synthesis minimizes the environmental footprint by using renewable natural resources (e.g., plant extracts, microorganisms) instead of hazardous chemicals.	[30]
Cost-Effective	The use of low-cost and easily accessible natural materials reduces the need for expensive chemicals and high-energy processes, making it suitable for large-scale production.	[31]
Enhanced Antimicrobial Activity	CuO nanoparticles synthesized through green methods demonstrate size-dependent antimicrobial properties, with smaller particles exhibiting stronger activity.	[32]
Simplicity and Scalability	Mild reaction conditions and natural materials simplify the process, making it scalable for industrial applications requiring large quantities of nanoparticles.	[33]
Control Over Nanoparticle Properties	Green synthesis allows control over the size, shape, and morphology of nanoparticles, which is crucial for applications in catalysis, sensors, and antimicrobial treatments.	[34]

Table 2. Disadvantages of green synthesis.

Disadvantages of Green Synthesis	Description	References
Limited Control Over Uniformity	Challenges exist in maintaining uniform size and morphology, which may affect the reproducibility and consistency of the nanoparticle properties across batches.	[35]
Slower Synthesis Rates	Green synthesis methods often have slower reaction rates compared to traditional chemical methods, limiting their applicability for high-throughput production.	[35]
Extraction Challenges	Extracting reducing agents from natural sources (e.g., plants, microbes) can pose difficulties related to consistency, yield, and production costs.	[35]
Antimicrobial Specificity	The antimicrobial activity of CuO nanoparticles may vary depending on the microorganism. For example, CuO nanoparticles may be more effective against bacteria than fungi.	[36]

This research explores two distinct approaches for the preparation of copper oxide (CuO) nanoparticles: a chemical approach using microwave- and ultrasound-assisted hydrolytic synthesis with copper acetate as the precursor and potassium hydroxide (KOH) as the hydrolyzing agent, and a green synthesis approach utilizing copper acetate as the precursor with egg white and tomato extract as the stabilizing and reducing agents. It is important to note that, in this study, egg white and *Solanum lycopersicum* extract were employed as separate variants for the green synthesis of CuO nanoparticles, rather than as a combination. Each of these natural materials offers specific advantages both as reducing agents and as templates for the formation and stabilization of nanoparticles.

Egg white albumin, frequently used in green synthesis, has shown promise as a stabilizer due to its biocompatibility and protein content, which can influence the morphology and size of the synthesized nanoparticles [10]. Additionally, tomato extract—a source of organic acids, sugars, and vitamins—has been used to stabilize nanoparticles, potentially enhancing their surface properties for specific applications, such as antibacterial activity [27].

2. Materials and Methods

2.1. Materials

Copper acetate dihydrate ($Cu(CH_3COOH)_2 \cdot 2H_2O$) with a purity of 99.8% was used as a precursor in both microwave- and ultrasound-assisted hydrolytic synthesis and green synthesis. The hydrolyzing agent, potassium hydroxide (KOH) pellets, and copper acetate were purchased from Sigma Aldrich, located in St. Louis, MO, USA. Green synthesis utilized cholesterol-free egg whites from free-range chickens and extract from *Solanum lycopersicum*. For each synthesis, a 0.5 M copper acetate solution was prepared by dissolving 9.08 g in 100 mL of demineralized water. *Solanum lycopersicum* was purchased from the local market in Pitești, Argeș County.

To prepare the broth, 500 g of peeled *Solanum lycopersicum* was boiled in 100 mL of demineralized water for 2 h and 30 min at a temperature of 75 °C until the liquid evaporated, and the desired consistency was achieved.

Preparation of Bacterial Cultures

To test the antibacterial properties of copper oxide powders, the following reference strains (qualitative, with an unknown number) were used: *Escherichia coli* ATCC 25922 and *Enterococcus faecalis* ATCC 19433 from IeLab (American Type Culture Collection, ATCC).

Bacterial load loops were each hydrated in 1 mL of sterile distilled water for 30 min at 37 °C. Using a sterile loop, passages were made on a non-selective medium, Tryptic Soy Agar, and incubated at 37 °C for 24 h. From these subcultures, working cultures were prepared in the same way. From the working cultures, bacterial loads were taken and transferred into 10 mL of sterile distilled water. To approximately determine the bacterial count, the McFarland densitometer was used. Knowing that 0.5 McFarland corresponds to a bacterial load of approximately 1.5×10^8 CFU/mL, the readings for the initial working suspensions were 0.31 McFarland for *Enterococcus faecalis* and 0.16 McFarland for *Escherichia coli*.

Since the densitometer may produce errors for readings below 0.5 McFarland, decimal dilutions were performed up to 10^{-3} for *Escherichia coli* and 10^{-4} for *Enterococcus faecalis*, followed by testing each dilution to determine the number of target bacteria, specifically the number of colonies developed which can be read on the culture medium. The culture media used were Merck Chromocult Coliform Agar and Slanetz and Bartley Agar.These were prepared according to the manufacturers' instructions: a 41.5 g/L concentration for Slanetz–Bartley Agar and 26.5 g/L for the Chromocult Coliform Agar medium, sterilized in

a water bath, allowed to reach a temperature of approximately 47–50 °C, and then poured into Petri dishes.

2.2. Chemical Synthesis of Nanostructured Copper Oxide

Nanostructured copper oxide was synthesized using a hydrolytic method enhanced by ultrasound and microwave techniques, with $Cu(CH_3COOH)_2 \cdot 2H_2O$ as the precursor and potassium hydroxide (KOH) as the hydrolyzing agent.

The process commenced with the preparation of a 0.5 M copper acetate solution (see Section 2.1) To precipitate the copper acetate, a 1 M KOH solution was gradually added under magnetic stirring at 500 rpm until the solution reached a pH of 11.

The resulting solution was transferred to a Berzelius beaker and subjected to sonication in a CD-4800 ultrasonic water bath for 10 min at a frequency of 42 kHz and a power of 60 W. This step facilitated particle dispersion through cavitation energy. Following sonication, the precipitate was exposed to microwave heating in a household oven (Samsung) at 850 W for 5 min, raising the solution temperature to approximately 85 °C.

To eliminate synthesis impurities, the precipitate was washed 10 times with deionized water. The washed sample was dried at 120 °C for 1 h, and the dried powder was subsequently calcined at 550 °C for 2 h. The calcination step is crucial, as it ensures the formation of the desired copper oxide phase, significantly affecting the powder's efficiency and properties.

This combination of ultrasonic and microwave techniques is particularly suitable for chemical synthesis involving inorganic precursors like copper acetate and KOH. The ultrasonic bath generates cavitation energy, which promotes a uniform particle dispersion, while microwave heating guarantees uniform and rapid thermal processing. Together, these methods enable precise control over the reaction rate and nanoparticle formation, yielding well-defined nanostructured copper oxide particles [22]

Figure 1 depicts the step-by-step process of the microwave- and ultrasound-assisted hydrolytic synthesis of nanostructured copper oxide, from the initial precursor solution to the final product.

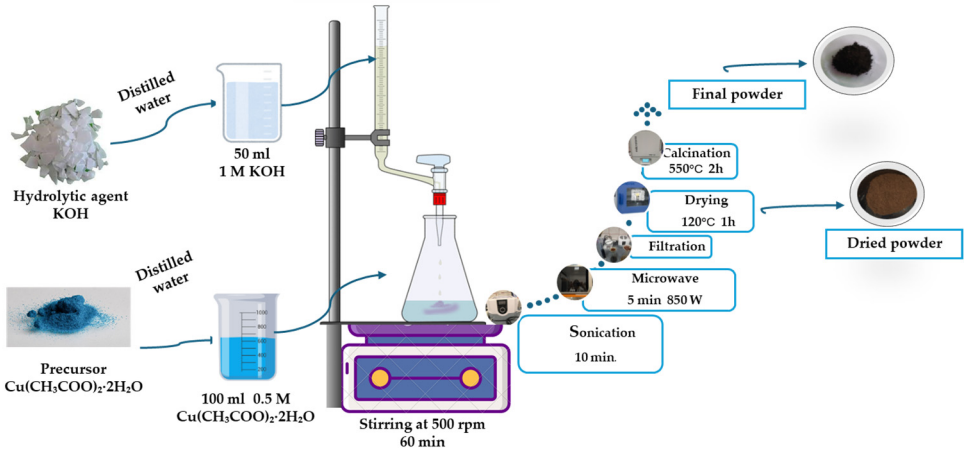


Figure 1. Flow diagram for the hydrolytic synthesis of nanostructured copper oxide assisted by microwave and ultrasound.

2.3. Green Synthesis of Nanostructured Copper Oxide

The green synthesis of nanostructured copper oxide utilized two distinct biological reductants: cholesterol-free egg white (albumin) and *Solanum lycopersicum* extract. In the first experiment, 100 mL of a 0.5 M $Cu(CH_3COOH)_2 \cdot 2H_2O$ solution was gradually added to 50 mL of egg white. In the second experiment, the same copper solution was combined with 50 mL of *Solanum lycopersicum* extract. Both mixtures were magnetically stirred at

500 rpm for 60 min at room temperature. The resulting products—a green solid in the case of albumin and a dark green precipitate in the case of *Solanum lycopersicum*—were filtered, washed with 400 mL of deionized water, dried at 120 °C for 2 h, and calcined at 550 °C for 2 h.

The objective of this green synthesis was to preserve the integrity and biological activity of the natural compounds used, such as the proteins from the egg white and the organic acids from *Solanum lycopersicum*. To achieve this, gentle methods like magnetic stirring at room temperature were selected, avoiding the high energies associated with techniques such as ultrasound- or microwave-assisted synthesis. For instance, the albumin in egg whites contains proteins rich in cysteine and methionine, which include thiol groups (-SH) which are crucial for reducing copper ions and stabilizing the nanoparticles [36]. These proteins are sensitive to high temperatures or aggressive processing, as denaturation would compromise their ability to stabilize and control nanoparticle growth [37]. Similarly, *Solanum lycopersicum* extracts contain organic acids and vitamins, such as citric acid and ascorbic acid, which play a key role in reducing copper ions and stabilizing the nanoparticles. High-energy techniques could degrade these compounds, diminishing the efficiency of green synthesis [35].

Each of these natural materials offers specific advantages both as a reducing agent and as a template for the formation and stabilization of nanoparticles.

Egg whites exhibita dual functionality in nanoparticle synthesis, acting as both stabilizing agents and reducing agents due to their rich protein content, particularly albumin. These proteins are abundant in functional groups, such as thiols (-SH) and amino groups ($-NH_2$), which facilitate the reduction of copper ions (Cu^{2+}) into nanoparticles while simultaneously serving as natural templates to stabilize the resulting structures. This dual functionality underscores the critical role of egg whites in both nanoparticle formation and structural control.However, due to the high viscosity of the solution, particle dispersion may be limited.

Solanum lycopersicum extract serves both reducing and stabilizing functions. This natural source is abundant in organic acids, such as citric acid and ascorbic acid, and is also a significant source of sugars and phenolic compounds. These components effectively reduce copper ions (Cu^{2+}) and function as stabilizers for the nanoparticles.

Figure 2 shows the step-by-step green synthesis process for the elaboration of nanostructured copper oxide.

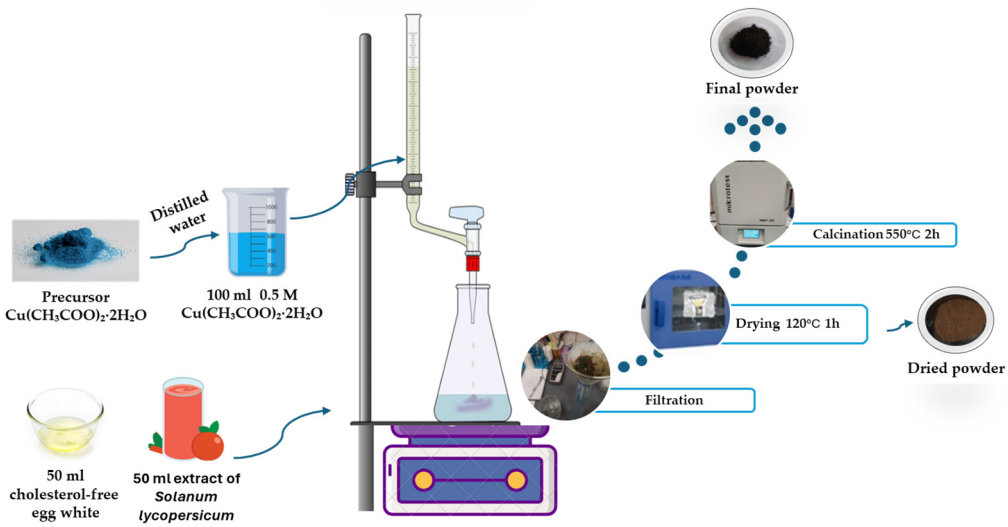


Figure 2. Flow diagram for the green synthesis of nanostructured copper.

2.4. Characterization of Nanostructured Copper Oxide

To perform morphological and structural studies on the nanostructured copper oxide developed through biochemical synthesis, various characterization techniques were employed. Among these techniques, powder X-ray diffraction in Bragg–Brentano geometry was performed using CuKα radiation (λ = 0.154 nm) at 45 kV and 40 mA, along with a one-dimensional D/teX Ultra detector equipped with a graphite monochromator. The X-ray diffractograms were recorded with CuKα radiation over a measuring range of 2θ: (28–105°), with a step size of 0.05° and a scanning speed of 2°/min, using the RIGAKU ULTIMA IV diffractometer. The XRD spectra were analyzed using the PDXL 2 program, and crystalline compounds were identified using the PDF 5+ database. Additionally, Fourier Transform Infrared (FTIR) spectra in the range of 350–4000 cm^{-1} with a resolution of 4 cm^{-1} were obtained using the Tensor 27 spectrometer. The HITACHI SU5000 Scanning Electron Microscope (SEM) was employed to examine particle morphology. The powder samples were spread on adhesive carbon tape and analyzed in variable-pressure mode (30 Pa), 25 kV acceleration voltage, and 127 μA emission current, at different magnifications.

2.5. Bacteriological Testing

For the bacteriological testing of copper oxide (CuO) powders on *Escherichia coli* and *Enterococcus faecalis*, a direct-contact method was employed, involving 0.015 g of each CuO powder mixed with a bacterial suspension prepared from the selected strains. The CuO powders were sterilized under a UV lamp for 15 min to ensure the absence of initial contamination. Artificial samples were created by mixing 18 mL of sterile distilled water with 0.1 mL of bacterial suspension. From each suspension, 1 mL of the sample was analyzed, which was estimated to contain approximately 100 CFU of *Enterococcus faecalis* and *Escherichia coli*, respectively. After a contact time of 24 h at 25 °C, destruction of the microorganisms was observed. Subsequently, a new inoculation of the samples was conducted with a higher number of microorganisms and a contact time of approximately 5 h, followed by incubation at 37 °C for 24 h, during which inhibition of microorganism growth was noted.

The initial working suspensions were prepared through serial decimal dilutions, resulting in a bacterial load of approximately 1.5×10^4 for *Escherichia coli* and 2×10^5 for *Enterococcus faecalis*.

Each sample was coded (CuO-1, CuO-2, and CuO-3). The positive control (M), used to ensure bacterial viability, consisted of sterile distilled water and bacterial suspension. The negative control, used to confirm sterility, consisted of sterile distilled water only. The CuO powders were immersed in the bacterial suspension for a short initial contact time (<30 min), after which the samples were immediately transferred to the selective culture medium, Chromocult Coliform Agar (CCA), to observe the effect on *E. coli*.

This approach, combining direct contact and incubation on selective media, allowed for the evaluation of the bactericidal and bacteriostatic effects of CuO powders.

3. Results and Discussions

3.1. XRD Analysis

3.1.1. Nanostructured Copper Oxide Prepared by Microwave- and Ultrasound-Assisted Hydrolytic Synthesis

XRD analysis confirmed the crystalline nature and phase structure of the chemically prepared nanostructured copper oxide. The two highest peaks in the XRD diffractogram were located at 2θ = 35.5° and 38.6°, accompanied by other peaks of lower intensity, as shown in Figure 3. These peaks corresponded to CuO with a monoclinic structure and a C12/c1 space group (ICCD PDF 5+ 2024 DB: 04-008-8215),consistent with those reported

in the literature [38]. The spectra showed an absence of Cu-bound peaks or other impurities, indicating the high purity of the prepared CuO nanoparticles. The average crystallite size (D) was determined to be 48 nm using the Williamson–Hall method [38]:

$$\beta COS\theta = K\lambda/D + 4\varepsilon sin\theta, \quad (1)$$

where β is the full-widt hhalf-maximum (FWHM)of the prominent peaks in the X-ray diffraction; K is the shape factor; λ is the X-ray wavelength (λ = 0.15418 nm); D is the particle size (D_{W-H}); and ε is the lattice strain of CuO nanoparticles.

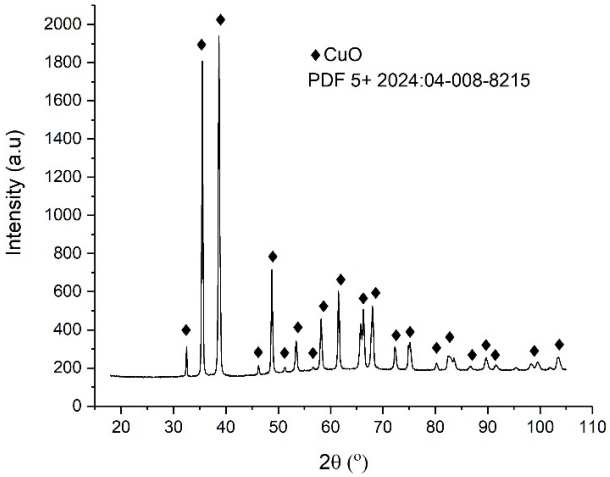


Figure 3. XRD pattern of nanostructured CuO prepared by microwave- and ultrasound-assisted hydrolytic synthesis, annealed at a temperature of 550 °C.

3.1.2. Nanostructured Copper Oxide Elaborated by Green Synthesis

Figure 4 shows overlapping spectra for nanostructured copper oxide synthesized using cholesterol-free egg whites and *Solanum lycopersicum* extract.

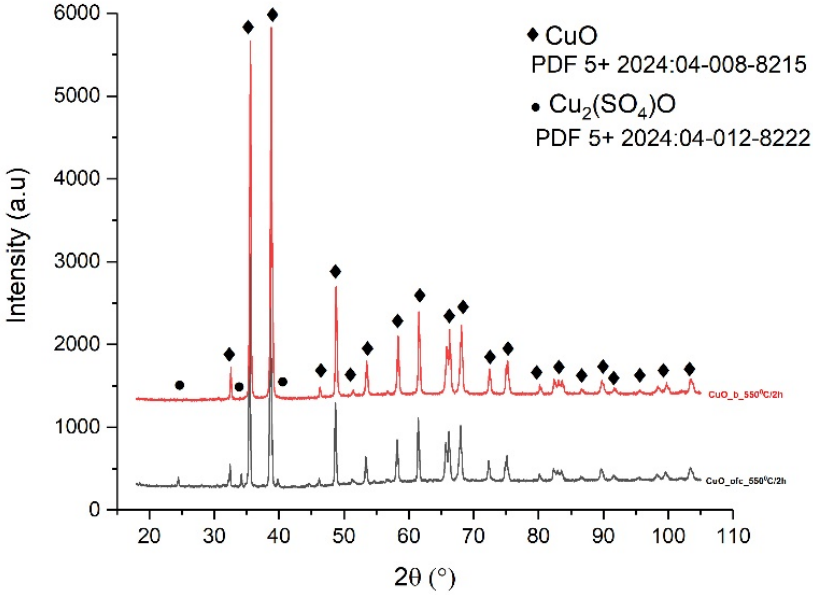


Figure 4. XRD patterns of copper oxide elaborated by green synthesis from egg whites and extract of *Solanum lycopersicum*.

In the CuO_ofc_550 °C/2h sample, the qualitative phase analysis revealed the presence of dolerophanite ($Cu_2(SO_4)O$) and tenorite (CuO). The formation of dolerophanite can be attributed to the interaction of copper with the sulfur compounds found in albumin,

which contains sulfur-containing amino acids like cysteine and methionine. Albumin is recognized for its capacity to bind metals, including copper, through the thiol (-SH) groups in cysteine and methionine. These interactions can result in the formation of sulfur compounds, such as copper sulfates. For instance, it has been noted that albumin forms complexes with transition metals, influencing their speciation in solution. Furthermore, cysteine and methionine are crucial in the biosynthesis of sulfur-containing amino acids, impacting metabolism and metal–sulfur interactions in organisms [39,40].

Studies in the literature support the hypothesis that the presence of dolerophannite in the analyzed sample results from the interaction of copper with sulfur-containing amino acids in albumin, leading to the formation of specific compounds like copper sulfates.

In the CuO_b_550 °C/2h sample, diffraction peaks corresponding to a single crystalline phase, CuO, with a monoclinic structure, were observed, in agreement with PDF5+2024 DB:04-008-8215. The average crystallite size was determined using the Williamson–Hall method, as shown in Table 3.

Table 3. Average crystallite size by Williamson–Hall method for CuO.

Sample Code	D (nm)
CuO_ofc_550/2h	59.6 ± 0.3
CuO_b_550/2h	53.7 ± 0.4

3.2. ATR-FTIR Analysis

3.2.1. Nanostructured Copper Oxide Prepared by Microwave- and Ultrasound-Assisted Hydrolytic Synthesis

To confirm CuO elaboration, ATR-FTIR analysis was performed with the Tensor 27 Bruker spectrometer, with 4 cm^{-1} resolution.

The ATR-FTIR spectrum of calcinated CuO at 550 °C was compared with the spectrum of commercial CuO, provided by Merk. The broad band around 3400 cm^{-1} was characteristic of O-H stretching vibrations, associated with water molecules or hydroxyl groups. The presence of this band suggests that the samples might have contained some adsorbed water or hydroxyl groups on the surface. Figure 5 shows strong band absorption at 434 cm^{-1} and another at 362 cm^{-1} due to the strong vibration of Cu-O [16,17].

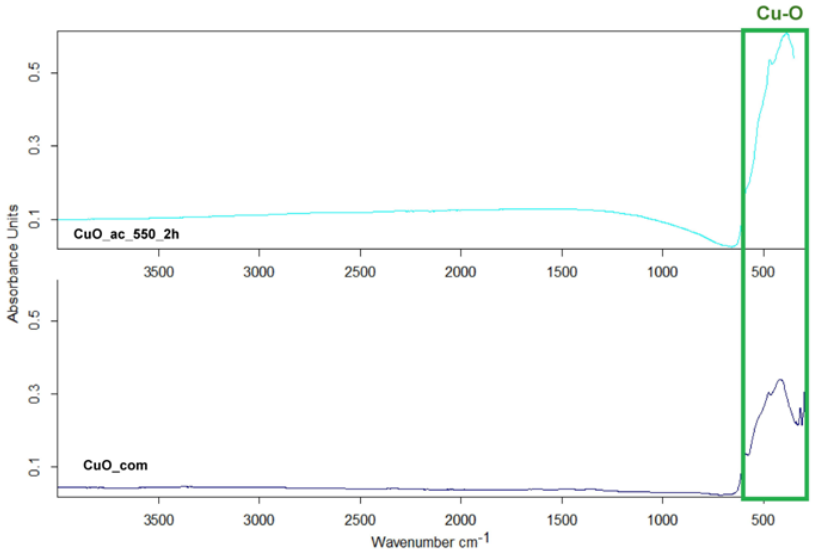


Figure 5. ATR-FTIR spectra of CuO_ac_550_2h powder compared to commercial CuO.

The intensity of the Cu-O peaks of CuO_ac_550_2h was significantly higher compared to commercial CuO, indicating a good crystalline structure of the elaborated particles

prepared by microwave- and ultrasound-assisted hydrolytic synthesis. No other band of absorption was attributed to CO_2 molecules from the air.

3.2.2. Nanostructured Copper Oxide Elaborated by Green Synthesis

The ATR-FTIR spectra of calcinated CuO_ofc_550/2h and CuO_b_550/2h were compared with the spectrum of commercial CuO powder, as presented in Figure 6.

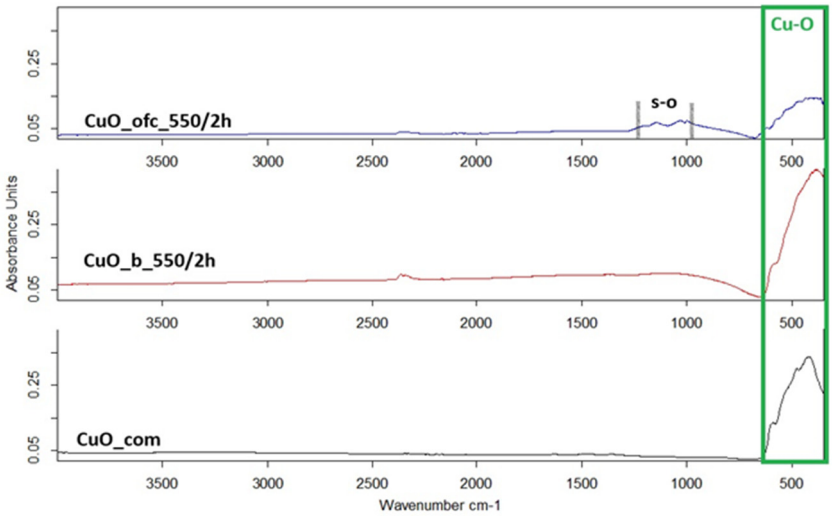


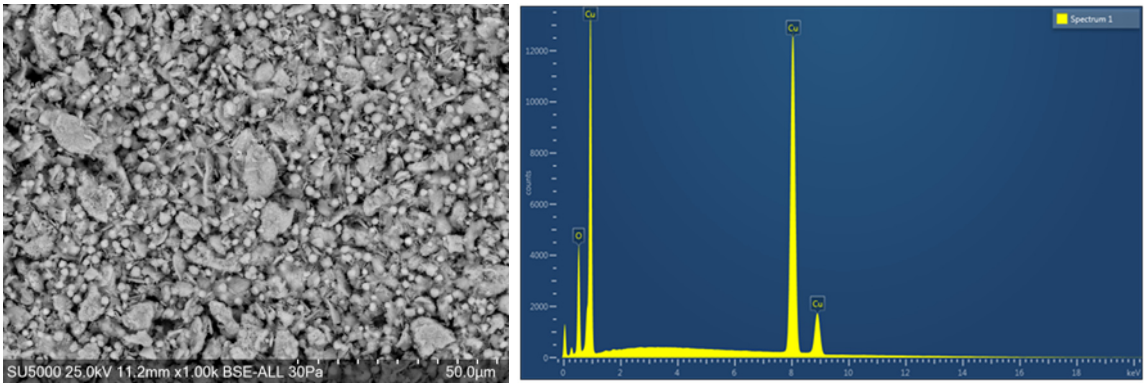
Figure 6. ATR-FTIR spectra ofcalcinated CuO_ofc_550/2h and CuO_b_550/2h compared to commercial CuO.

The broad band around 3400 cm^{-1} characteristic of O-H stretching vibrations was associated with water molecules or hydroxyl groups absorbed on the surface. The sharp peak around 434 cm^{-1} was indicative of a Cu-O bond. The Cu-O peak intensities varied across the spectra due to the crystallinity of the samples [16]. The CuO elaborated by green chemistry using *Solanum lycopersicum* extract was proven to be more crystalline than the CuO elaborated using cholesterol-free egg whites. In the range of 1200–1998 cm^{-1}, a stronger S-O bond was observed only in CuO elaborated using cholesterol-free egg whites, in accordance with XRD analysis. This presence of the S-O bond was attributed to SO_3 vibration. The presence of S was due to amino acids in the egg white: cysteine or methionine. Only in the CuO_b_550 /2h spectrum, the vibrations of C-O in the region 2359–2341 cm^{-1} indicated the presence of CO_2 molecules in the air [17].

3.3. SEM- EDS Analysis

3.3.1. Nanostructured Copper Oxide Elaborated by Microwave- and Ultrasound-Assisted Hydrolytic Synthesis

The morphology of the prepared CuO particles was examined using scanning electron microscopy (SEM). As shown in Figure 7a, the SEM images demonstrated two distinct morphologies of CuO nanoparticles: sheet-like and microspherical morphologies. Three characteristic intense peaks were observed for copper at 1 keV, 8.1 keV, and 9 keV, along with another peak at 0.6 keV attributed to oxygen. The EDS analysis of CuO, shown in Figure 7b, confirmed that the prepared powder sample contained two components, Cu and O, with weight percentages of 85.61 wt% copper and 14.39 wt% oxygen, as detailed in Table 4. The synthesis was performed using copper acetate and potassium hydroxide, and no other elements were detected. This result was attributed to the intermediate product ($Cu(OH)_2$) being washed several times with deionized water and calcined at 550 °C for 2 h.



(**a**) (**b**)

Figure 7. (**a**) SEM micrographs of CuO calcined at 550 °C for 2 h and (**b**) EDS spectrum of CuO developed by microwave- and ultrasound-assisted hydrolytic synthesis.

Table 4. Elemental composition of copper oxide.

Element	Wt%	Wt% Sigma
O	14.39	±0.12
Cu	85.61	±0.12

3.3.2. Nanostructured Copper Oxide Produced by Green Synthesis

Figure 8a reveals the presence of larger agglomerated particles of an irregular shape. This morphology suggests particle growth, likely influenced by the high viscosity of the egg white, which limits particle dispersion. Rich in proteins such as albumin, egg whites serve both as stabilizing and shaping agents, facilitating nucleation and growth. This protein-mediated mechanism may favor the formation of these larger clusters by promoting binding between particles, thereby contributing to the observed morphology.

The presence of albumin introduces functional groups such as thiols (-SH), amines (-NH_2), and carboxyl (-COOH), which can interact with Cu^{2+}, promoting reduction and stabilization during the synthesis process. These interactions are crucial for controlling nanoparticle nucleation and growth rates. However, the high protein content and viscosity of egg whites create a crowded environment that may lead to the limited diffusion of nanoparticles, favoring agglomeration over individual particle dispersion [36,37]. Furthermore, the cysteine and methionine residues in albumin, which contain sulfur, can bind strongly to the surface of forming nanoparticles, acting as nucleation sites. These sulfur-containing amino acids are known to influence particle morphology, encouraging cluster formation through bridging interactions between adjacent nanoparticles. Such interactions may explain the observed larger and irregularly shaped agglomerates. Additionally, the presence of hydrogen bonding and hydrophobic interactions within the protein matrix can contribute to particle binding and aggregation [37]. As the reaction progresses, these protein-mediated mechanisms lead to the formation of larger, less uniform clusters, which are consistent with the morphologies observed. This protein-driven process aligns with previous studies, which report that high-protein environments tend to favor agglomeration due to steric hindrance and reduced particle mobility [35]. However, these aggregates can exhibit enhanced stability due to the protective layer formed by adsorbed proteins, which may also influence the nanoparticles' surface properties and potential applications [35].

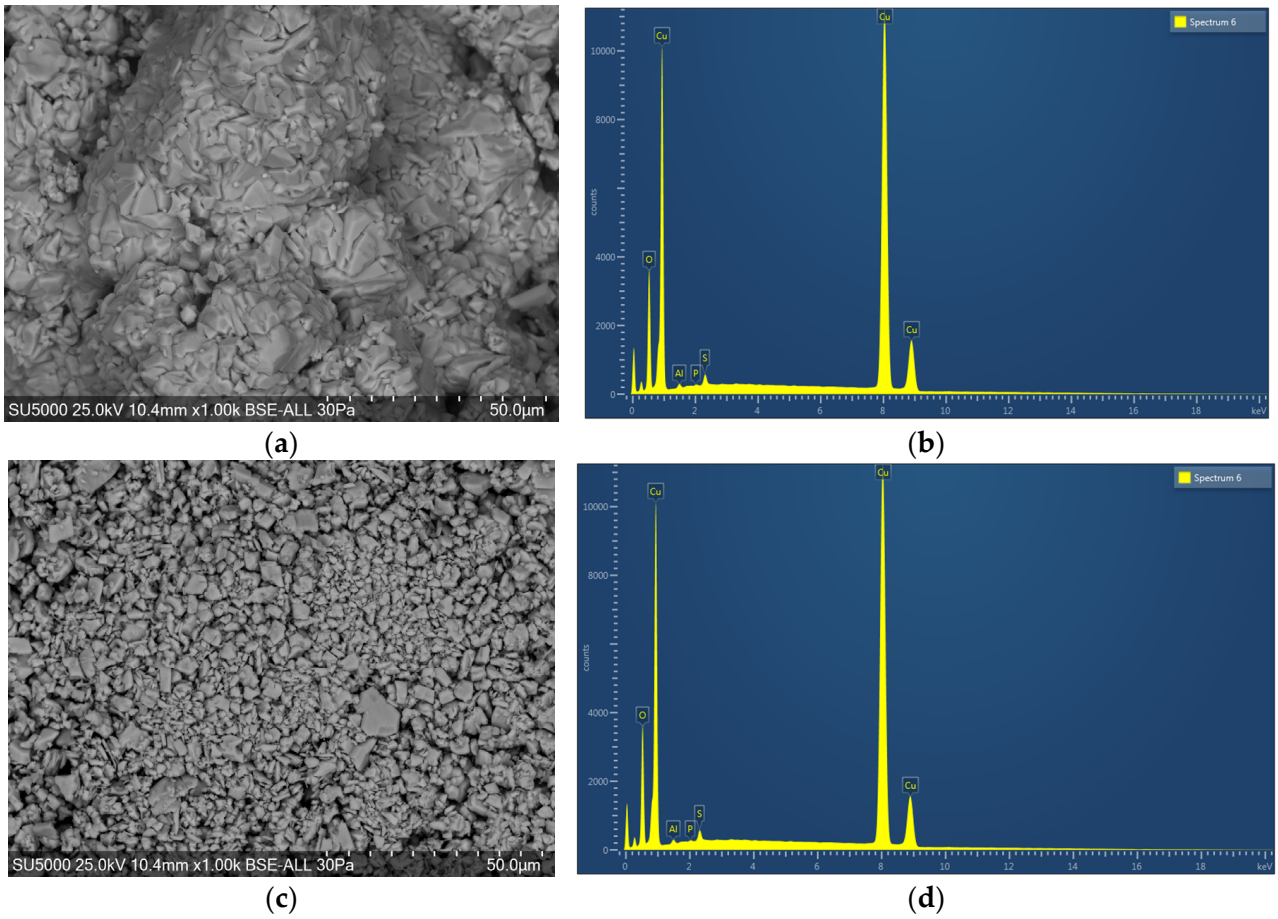


Figure 8. (**a**) SEM image of CuO prepared by green synthesis from cholesterol-free egg white; (**b**) EDS spectra of CuO prepared by green synthesis from cholesterol-free egg white; (**c**) SEM image of CuO prepared by green synthesis from *Solanum lycopersicum* extract; and (**d**) EDS spectra of CuO prepared by green synthesis from *Solanum lycopersicum* extract.

Figure 8b represents the EDS (energy-dispersive spectroscopy) spectra, where two large and prominent peaks can be observed around the energies of 1 keV and 8 keV. According to Table 3, copper accounts for 85.26 wt% of the composition by weight, which is consistent with copper oxide being the main product of the synthesis. The peak associated with oxygen is observed at low energy values around 0.5 keV, where oxygen is present at 13.56%, indicating the formation of copper oxide (CuO). The presence of oxygen is expected since copper oxide is the primary compound resulting from the reaction. Aluminum appears as a small peak in the spectrum, at about 1.5 keV, with a very low composition of 0.43%. This may be an incidental impurity from the equipment or the synthesis medium. Additionally, a very small peak for phosphorus is observed at about 2 keV, showing an extremely low presence of 0.10%. This could originate from egg whites, which contain phospholipids and other organic compounds. The EDS spectrum also displays a small peak around 2.3 keV, corresponding to the 0.65% attributed to sulfur. The presence of this element can be explained using egg white, which contains cysteine-rich, sulfur-containing proteins. Table 5 shows the composition of the copper oxide prepared by the green synthesis of copper acetate and cholesterol-free egg white.

Table 5. Elemental composition of copper oxide prepared by green synthesis.

Element	Wt%	Wt% Sigma
CuO prepared by green synthesis from cholesterol-free egg white		
O	13.56	±0.12
Al	0.43	±0.04
P	0.10	±0.03
S	0.65	±0.03
Cu	85.26	±0.14
Total	100.00	
CuO prepared by green synthesis from *Solanum lycopersicum* extract		
O	16.15	±0.12
Al	0.41	±0.04
P	0.13	±0.03
S	0.19	±0.03
Cu	83.12	±0.13
Total	100.00	

Figure 8c shows a finer and more uniform distribution of copper oxide particles.

The particles, which take the form of irregular polyhedra, are more dispersed compared to the copper oxide obtained from egg white. This morphology indicates that the tomato extract promotes the formation of finer particles, likely due to its acidic environment, which is rich in organic acids (such as citric acid and ascorbic acid) and smaller, low-molecular-weight compounds that act as stabilizing agents. The presence of acids and the lower viscosity of the tomato extract allow for the better dispersion of particles, resulting in more evenly distributed CuO particles with reduced aggregation.

Figure 8d represents the EDS spectra, revealing prominent peaks for copper at approximately 1 keV and 8 keV, consistent with the findings from the previous spectrum, indicating a high concentration of copper. According to Table 5, copper constitutes 83.12% of the composition, further confirming that the synthesis resulted in a copper-rich compound. A small peak for oxygen is observed at approximately 0.5 keV, mirroring the previous spectrum, with oxygen present at 16.15%, which supports the formation of copper oxide (CuO). The presence of oxygen is crucial for confirming the existence of the metal oxide compound. As seen in the earlier spectrum, a minor peak for aluminum appears around 1.5 keV, indicating a low concentration of 0.41%. This may represent an impurity introduced from laboratory equipment or the surrounding environment. Phosphorus is detected in the spectrum at approximately 2 keV, with a composition of 0.13%, likely originating from organic compounds present in the *Solanum lycopersicum* extract. Additionally, a small peak associated with sulfur is identified around 2.3 keV, indicating a presence of 0.19%. Given that plants can contain trace amounts of sulfur, this may also be attributed to impurities from the *Solanum lycopersicum* extract.

The results confirm that green synthesis introduces variability in particle morphology due to the complex nature of biological extracts. However, these variations can enhance the functional properties, such as reactivity or antibacterial efficacy, highlighting the adaptability of green methods compared to the precision of chemical synthesis.

4. Antibacterial Properties of CuO

From Table 6, it can be observed that, with a contact time of less than 30 min, all three CuO samples demonstrate a significant reduction in the bacteria *Escherichia coli* compared to the control sample. The CuO_1 sample showed the best results, followed by the CuO_2 sample, while the CuO_3 sample was the least effective of the three. This suggests that all CuO samples had an initial bacteriostatic effect, inhibiting the rapid

multiplication of bacteria. After 24 h of contact, all CuO samples completely inhibited bacterial growth (0 CFU, colony-forming units for both types of bacteria), indicating a strong long-term bactericidal effect. These results demonstrate that CuO can eliminate bacteria under prolonged contact conditions.

Table 6. Antibacterial properties of CuO.

Tested Samples	Sample Code	Contact Time (<30 min)	Contact Time (24 h)		Added Bacterial Load Contact Time (5 h)	
		Escherichia coli CFU/0.5 mL	*Enterococci* CFU/1 mL	*Escherichia coli* CFU/1 mL	*Enterococci* CFU/1 mL	*Escherichia coli* CFU/1 mL
Martor	M	60	~100	~100	~500	~150
CuO_ofc_0.5M_2h	CuO_1	2	0	0	10	0
CuO_b_0.5M_2h	CuO_2	12	0	0	40	0
CuO_ac_550_2h	CuO_3	26	0	0	150	1

The green-synthesized nanoparticles may have possessed a more hydrophilic surface due to the presence of -OH and -COOH groups, which enhanced their adhesion and activity against both Gram-negative and Gram-positive bacteria. Similar results were reported by Vaidehi et al. in their study on copper oxide nanoparticles synthesized using *Solanum lycopersicum* leaf extract [41]. They observed significant antibacterial and photocatalytic activity of CuO nanoparticles, demonstrating a strong bactericidal effect against *Escherichia coli* and other strains under prolonged exposure.Under high bacterial loads and a contact time of 5 h, differences in the efficiency of the three samples were observed. Thus, the CuO_1 sample proved to be the most effective, managing to maintain a very low number of colonies of *Escherichia coli* and eliminating *Enterococcus faecalis.* The CuO_2 sample was slightly less effective, allowing for a slight increase in *Enterococcus faecalis* while keeping *Escherichia coli* at 0 CFU. The CuO_3 sample allowed for a greater increase in *Enterococcus faecalis* and a small presence of *E. coli*, suggesting a reduced antibacterial efficiency under high bacterial loads.

5. Conclusions

Two effective methods for CuO synthesis were presented in this study: microwave- and ultrasound-assisted hydrolytic synthesis using copper acetate and KOH, and green-synthesis utilizing cholesterol-free egg white albumin and tomato extract. Each method yielded nanostructured CuO with unique characteristics. The application of multiple characterization techniques, including XRD, FTIR, and SEM-EDS, confirmed the crystalline structure and high purity of the CuO synthesized via microwave- and ultrasound-assisted hydrolysis. The XRD results indicated a monoclinic phase, validating the successful formation of tenorite (CuO). In the green synthesis approach for the CuO_ofc_550 °C/2 h sample, additional phases, such as dolerophanite ($Cu_2(SO_4)O$), were detected, likely owing to the presence of sulfur compounds in the albumin. The average crystallite sizes were determined to be 59.6 ± 0.3 nm for CuO_ofc_550 °C/2 h, 53.7 ± 0.4 nm for CuO_b_550 °C/2 h, and 48 ± 0.2 nm for another CuO sample, as calculated using the Williamson–Hall method. The ATR-FTIR analysis performed on the calcined CuO samples provided valuable insights into their structural characteristics. The prominent bands observed around 3400 cm^{-1}, linked to O-H stretching, indicated the presence of adsorbed water or hydroxyl groups on the surface, while the strong absorption peaks at 434 cm^{-1} confirmed the formation of Cu-O bonds. The increased intensity of Cu-O peaks in the CuO synthesized through microwave- and ultrasound-assisted hydrolytic methods, particularly when using *Solanum lycopersicum* extract, suggested a superior crystalline structure compared to commercial

CuO. Furthermore, the detection of an S-O bond in the spectrum of CuO synthesized with cholesterol-free egg white indicated the influence of amino acids such as cysteine or methionine, contributing to the distinct chemical environment of the prepared materials. Notably, the presence of CO_2 was exclusively observed in one sample, further distinguishing the methodologies employed. Overall, the findings highlight the effectiveness of green chemistry approaches in developing crystalline CuO, with implications for its applications across various fields.

The morphology of CuO nanoparticles varied significantly depending on the synthesis method. The synthesis environment influenced the size and agglomeration of CuO particles.The hydrolytic synthesis produced sheet-like and microspherical nanoparticles, while green synthesis yielded finer and more uniformly distributed polyhedral particles. Egg white, rich in proteins, resulted in larger agglomerated particles, while the tomato extract, with its lower viscosity and acidic environment, facilitated the formation of smaller, more evenly distributed particles. These findings emphasize the importance of selecting appropriate stabilizing agents in the synthesis process, as variability in morphology can influence the performance of CuO in various applications.

All three CuO samples exhibited significant antibacterial properties, demonstrating a rapid bacteriostatic effect and a long-term bactericidal effect against *Escherichia coli* and *Enterococcus faecalis*. However, their efficiency varied depending on the synthesis conditions, so certain formulations (such as CuO_1) were more effective in inhibiting bacteria, even under high bacterial loads.

In view of its potent antibacterial properties and the feasibility of environmentally friendly synthesis methods, nanostructured copper oxide holds significant potential for applications across various fields, including medicine, environmental science, and material engineering. Further research is essential to explore the scalability of these synthesis methods and investigate the long-term stability and efficacy of CuO nanoparticles in environmental applications.

Author Contributions: Conceptualization, A.-G.S. and E.M.M.; methodology, A.-G.S.; software, I.C.; validation, A.-G.S.; formal analysis, D.A.N. and S.G.M.; investigation, E.M.M., D.A.N., D.I. and I.C.; resources, E.M.M.; data curation, A.-G.S.; writing—original draft preparation, E.M.M.; writing—review and editing, A.-G.S., E.M.M., D.A.N. and S.G.M.; visualization, M.O.; and supervision, A.-G.S. All authors have read and agreed to the published version of the manuscript.

Funding: This research received no external funding.

Data Availability Statement: Data is contained within the article.

Conflicts of Interest: The authors declare no conflicts of interest.

References

1. Bishwakarma, H.; Anand, M.; Das, A.K. Strategies for Synthesizing Metal Oxide Nanoparticles and the Challenges. In *Advanced Materials and Nano Systems: Theory and Experiment (Part 3)*; Rai, D.P., Obodo, K.O., Singh, J.P., Eds.; Bentham Science Publishers: Sharjah, United Arab Emirates, 2024; pp. 260–282; ISBN 978-981-5223-10-1.
2. Li, Y.; Tang, N.; Zhao, L.; Bao, X.; Wang, Y.; Wang, Z.; Hu, M. Copper-Based Nanodots as Efficient Biomimetic Antibiotics for the Treatment of Oral Bacterial Infections. *Particuology* **2024**, *91*, 190–201. [CrossRef]
3. Negrescu, A.M.; Killian, M.S.; Raghu, S.N.V.; Schmuki, P.; Mazare, A.; Cimpean, A. Metal Oxide Nanoparticles: Review of Synthesis, Characterization and Biological Effects. *J. Funct. Biomater.* **2022**, *13*, 274. [CrossRef]
4. Doicin, I.E.; Neacsu, I.A.; Ene, V.L.; Birca, A.C.; Andronescu, E. Development and characterization of sodium alginate-ZnO nanoparticle reinforced composites for biomedical applications. *UPB Sci. Bull.* **2024**, *86*, 157–167.
5. Ananth, A.; Dharaneedharan, S.; Heo, M.-S.; Mok, Y.S. Copper Oxide Nanomaterials: Synthesis, Characterization and Structure-Specific Antibacterial Performance. *Chem. Eng. J.* **2015**, *262*, 179–188. [CrossRef]
6. Khan, I.; Saeed, K.; Khan, I. Nanoparticles: Properties, Applications and Toxicities. *Arab. J. Chem.* **2019**, *12*, 908–931. [CrossRef]

7. Akarken, G.; Cengiz, U.; Bektaş, T.E. Hydrothermal Synthesis of CuO Nanoparticles: Tailoring Morphology and Particle Size Variations for Enhanced Properties. *J. Adv. Res. Nat. Appl. Sci.* **2024**, *10*, 329–336. [CrossRef]
8. Salman, K.D.; Abbas, H.H.; Aljawad, H.A. Synthesis and Characterization of MgO Nanoparticle via Microwave and Sol-Gel Methods. *J. Phys. Conf. Ser.* **2021**, *1973*, 012104. [CrossRef]
9. Nahar, B.; Chaity, S.B.; Gafur, M.A.; Hossain, M.Z. Synthesis of Spherical Copper Oxide Nanoparticles by Chemical Precipitation Method and Investigation of Their Photocatalytic and Antibacterial Activities. *J. Nanomater.* **2023**, *2023*, 2892081. [CrossRef]
10. Zou, Y.-L.; Li, Y.; Li, J.-G.; Xie, W.-J. Hydrothermal Synthesis of Momordica-like CuO Nanostructures Using Egg White and Their Characterisation. *Chem. Pap.* **2012**, *66*, 278–283. [CrossRef]
11. Labanni, A.; Nasir, M.; Arief, S. Research Progress and Prospect of Copper Oxide Nanoparticles with Controllable Nanostructure, Morphology, and Function via Green Synthesis. *Mater. Today Sustain.* **2023**, *24*, 100526. [CrossRef]
12. Jain, K.; Takuli, A.; Gupta, T.K.; Gupta, D. Rethinking Nanoparticle Synthesis: A Sustainable Approach vs. Traditional Methods. *Chem. Asian J.* **2024**, *19*, e202400701. [CrossRef]
13. Alzalzala, S.; Al-Shamari, A.M.J. Preparation and Characterization of Copper Oxide CuO (II) Nanoparticles Prepared by a Hydrothermal Method and for Solar Cells Applications. *J. Kufa-Phys.* **2023**, *15*, 108–116. [CrossRef]
14. Dörner, L.; Cancellieri, C.; Rheingans, B.; Walter, M.; Kägi, R.; Schmutz, P.; Kovalenko, M.V.; Jeurgens, L.P.H. Cost-Effective Sol-Gel Synthesis of Porous CuO Nanoparticle Aggregates with Tunable Specific Surface Area. *Sci. Rep.* **2019**, *9*, 11758. [CrossRef] [PubMed]
15. Shanan, Z.J.; Hadi, S.M.; Shanshool, S.K. Structural Analysis of Chemical and Green Synthesis of CuO Nanoparticles and Their Effect on Biofilm Formation. *Baghdad Sci. J.* **2018**, *15*, 0211. [CrossRef]
16. Phiwdang, K.; Suphankij, S.; Mekprasart, W.; Pecharapa, W. Synthesis of CuO Nanoparticles by Precipitation Method Using Different Precursors. *Energy Procedia* **2013**, *34*, 740–745. [CrossRef]
17. Pookmanee, P.; Sangthep, P.; Tafun, J.; Kruefu, V.; Kojinok, S.; Phanichphant, S. Synthesis, Characterization and Its Photocatalytic of Copper Oxide (CuO) Powder. *Mater. Sci. Forum* **2019**, *962*, 70–76. [CrossRef]
18. Kaushal, S.; Bansal, S.; Prakash, C.; Singh, B.; Gupta, D. *Green Manufacturing and Materials Processing Methods: Characterizations, Applications, and Design*, 1st ed.; CRC Press: Boca Raton, FL, USA, 2024; ISBN 978-1-00-344922-5.
19. Liu, Y.; Biswas, B.; Hassan, M.; Naidu, R. Green Adsorbents for Environmental Remediation: Synthesis Methods, Ecotoxicity, and Reusability Prospects. *Processes* **2024**, *12*, 1195. [CrossRef]
20. Santhanaraj, G.; Alagarsamy, M.; Vedhi, C. *Microwave-Assisted Synthesis and Characterization of Metal Oxide Nanoparticles for Biological and Electrochemical Applications*; Research Square R&D LLC: Durham, NC, USA, 2024.
21. Rajamohan, R.; Lee, Y.R. Microwave-Assisted Synthesis of Copper Oxide Nanoparticles by Apple Peel Extract and Efficient Catalytic Reduction on Methylene Blue and Crystal Violet. *J. Mol. Struct.* **2023**, *1276*, 134803. [CrossRef]
22. Rai, R.S.; Bajpai, V. Growth of CuO Nanoparticles Using One Step Chemical Bath Deposition under Microwave Heating and Their Characterizations. *Int. J. Mater. Res.* **2023**, *114*, 335–343. [CrossRef]
23. Ahmed, M.A.; Mohamed, A.A. Advances in Ultrasound-Assisted Synthesis of Photocatalysts and Sonophotocatalytic Processes: A Review. *iScience* **2024**, *27*, 108583. [CrossRef]
24. Sarkar, P. Ultrasound-Assisted Green Synthesis of Nanoparticles and Their Applications. *Int. J. Sci. Res. Sci. Technol.* **2022**, *9*, 197–202. [CrossRef]
25. Morin, J.; Fujimoto, K.; Preston, A.; Guillen, D.P. Synthesis Methods for Nanoparticle Morphology Control in Energy Applications. In *REWAS 2022: Energy Technologies and CO_2 Management*; Tesfaye, F., Zhang, L., Guillen, D.P., Sun, Z., Baba, A.A., Neelameggham, N.R., Zhang, M., Verhulst, D.E., Alam, S., Eds.; The Minerals, Metals & Materials Series; Springer International Publishing: Cham, Switzerland, 2022; Volume II, pp. 21–31; ISBN 978-3-030-92558-1.
26. Pawar, A.; Mungole, A.; Naktode, K. Biogenic Copper Oxide Nanoparticles Synthesized from Whole Plant Extract of Nicotiana Plumbaginifolia Viv.: Characterization, Antibacterial, and Antioxidant Properties. *J. Turk. Chem. Soc. Sect. A Chem.* **2024**, *11*, 1005–1016. [CrossRef]
27. Gebreslassie, Y.T.; Gebremeskel, F.G. Green and Cost-Effective Biofabrication of Copper Oxide Nanoparticles: Exploring Antimicrobial and Anticancer Applications. *Biotechnol. Rep.* **2024**, *41*, e00828. [CrossRef] [PubMed]
28. Bansal, A. (Ed.) *Recent Developments in Science and Technology for Sustainable Future*; B P International: West Bengal, India, 2024; ISBN 978-81-970279-3-2.
29. Dargah, M.M.; Pedram, P.; Cabrera-Barjas, G.; Delattre, C.; Nesic, A.; Santagata, G.; Cerruti, P.; Moeini, A. Biomimetic Synthesis of Nanoparticles: A Comprehensive Review on Green Synthesis of Nanoparticles with a Focus on Prosopis Farcta Plant Extracts and Biomedical Applications. *Adv. Colloid Interface Sci.* **2024**, *332*, 103277. [CrossRef]
30. Araya-Castro, K.; Chao, T.-C.; Durán-Vinet, B.; Cisternas, C.; Ciudad, G.; Rubilar, O. Green Synthesis of Copper Oxide Nanoparticles Using Protein Fractions from an Aqueous Extract of Brown Algae Macrocystis Pyrifera. *Processes* **2020**, *9*, 78. [CrossRef]
31. Amin, F.; Fozia; Khattak, B.; Alotaibi, A.; Qasim, M.; Ahmad, I.; Ullah, R.; Bourhia, M.; Gul, A.; Zahoor, S.; et al. Green Synthesis of Copper Oxide Nanoparticles Using Aerva Javanica Leaf Extract and Their Characterization and Investigation of In Vitro Antimicrobial Potential and Cytotoxic Activities. *Evid.-Based Complement. Altern. Med.* **2021**, *2021*, 5589703. [CrossRef] [PubMed]

32. Nzilu, D.M.; Madivoli, E.S.; Makhanu, D.S.; Wanakai, S.I.; Kiprono, G.K.; Kareru, P.G. Green Synthesis of Copper Oxide Nanoparticles and Its Efficiency in Degradation of Rifampicin Antibiotic. *Sci. Rep.* **2023**, *13*, 14030. [CrossRef]
33. Ramasubbu, K.; Padmanabhan, S.; Al-Ghanim, K.A.; Nicoletti, M.; Govindarajan, M.; Sachivkina, N.; Rajeswari, V.D. Green Synthesis of Copper Oxide Nanoparticles Using Sesbania Grandiflora Leaf Extract and Their Evaluation of Anti-Diabetic, Cytotoxic, Anti-Microbial, and Anti-Inflammatory Properties in an In-Vitro Approach. *Fermentation* **2023**, *9*, 332. [CrossRef]
34. Sankara Narayanan, V.P.; Kathirason, S.G.; Elango, P.; Subramanian, R.; Sivagurusundar, R.; Gurusamy, A. Emilia Sonchifolia Leaf Extract-Mediated Green Synthesis, Characterization, In Vitro Biological Activities, Photocatalytic Degradation and in Vivo Danio Rerio Embryo Toxicity of Copper Nanoparticles. *RSC Adv.* **2023**, *13*, 16724–16740. [CrossRef] [PubMed]
35. Gupta, Y.; Rai, V.; Singh, A.; Khan, S.; Bano, N.; Yadav, R. The Uniqueness of Albumin as a Carrier in Nano Drug Delivery. *J. Res. Appl. Sci. Biotechnol.* **2024**, *3*, 7–11. [CrossRef]
36. Nicoud, L.; Lattuada, M.; Yates, A.; Morbidelli, M. Impact of Aggregate Formation on the Viscosity of Protein Solutions. *Soft Matter* **2015**, *11*, 5513–5522. [CrossRef] [PubMed]
37. Azizi, M.; Ghourchian, H.; Yazdian, F.; Dashtestani, F.; AlizadehZeinabad, H. Cytotoxic Effect of Albumin Coated Copper Nanoparticle on Human Breast Cancer Cells of MDA-MB 231. *PLoS ONE* **2017**, *12*, e0188639. [CrossRef] [PubMed]
38. Khuram, A.; Muhammad, S.; Suriani, A.B.; Younus, A.; Hassan, A.; Muhammad, Z.R. Synthesis of copper oxide (CuO) via coprecipitation method: Tailoring structural and optical properties of CuO nanoparticles for optoelectronic device applications. *Hybrid Adv.* **2024**, *6*, 100250. [CrossRef]
39. Wirtz, M.; Droux, M. Synthesis of the Sulfur Amino Acids: Cysteine and Methionine. *Photosynth. Res.* **2005**, *86*, 345–362. [CrossRef]
40. Klein, J. Probing the Interactions of Proteins and Nanoparticles. *Proc. Natl. Acad. Sci. USA* **2007**, *104*, 2029–2030. [CrossRef] [PubMed]
41. Vaidehi, D.; Bhuvaneshwari, V.; Bharathi, D.; Sheetal, B.P. Antibacterial and Photocatalytic Activity of Copper Oxide Nanoparticles Synthesized Using Solanum Lycopersicum Leaf Extract. *Mater. Res. Express* **2018**, *5*, 085403. [CrossRef]

Disclaimer/Publisher's Note: The statements, opinions and data contained in all publications are solely those of the individual author(s) and contributor(s) and not of MDPI and/or the editor(s). MDPI and/or the editor(s) disclaim responsibility for any injury to people or property resulting from any ideas, methods, instructions or products referred to in the content.